

Anomalous metallic state above the upper critical field of the conventional three-dimensional superconductor AgSnSe_2 with strong intrinsic disorder

Zhi Ren, M. Kriener, A. A. Taskin, Satoshi Sasaki, Kouji Segawa, and Yoichi Ando*

Institute of Scientific and Industrial Research, Osaka University, Ibaraki, Osaka 567-0047, Japan

(Received 6 November 2012; published 28 February 2013)

We report superconducting properties of AgSnSe_2 , which is a conventional type II superconductor in the very dirty limit due to intrinsically strong electron scatterings. While this material is an isotropic three-dimensional (3D) superconductor with a not-so-short coherence length where strong vortex fluctuations are *not* expected, we found that the magnetic-field-induced resistive transition at fixed temperatures becomes increasingly broader toward zero temperature and, surprisingly, that this broadened transition is taking place largely *above* the upper critical field determined thermodynamically from the specific heat. This result points to the existence of an anomalous metallic state possibly caused by quantum phase fluctuations in a strongly disordered 3D superconductor.

DOI: [10.1103/PhysRevB.87.064512](https://doi.org/10.1103/PhysRevB.87.064512)

PACS number(s): 74.62.En, 74.25.Dw, 74.40.-n, 74.70.Dd

I. INTRODUCTION

The interplay between disorder and superconductivity has attracted sustained interest over the past few decades. In BCS superconductors, according to Anderson's theorem,¹ the superconducting critical temperature T_c and the energy gap Δ remain unaffected by the presence of weak disorder, although in unconventional superconductors both T_c and Δ are strongly suppressed with weak disorder.² In the strongly disordered regime, things become interesting even in BCS superconductors: In two-dimensional (2D) systems, strong disorder leads to a universal superconductor-to-insulator transition at a critical sheet resistance of $\sim h/4e^2$;^{3–10} furthermore, it has been found that, as T tends to zero, there emerges a broad range of magnetic field where the resistivity remains finite but is much smaller than the normal-state value, which arguably signifies the importance of quantum phase fluctuations.^{11,12} In three-dimensional (3D) systems, strong disorder leads to a disruption of the global superconducting coherence through reductions in both the superfluid density n_s and pairing interactions, which results in the superconducting order parameter to spatially fluctuate and gives rise to anomalous electronic states near the superconductor-to-metal transition.^{13,14} Experimentally, while the 2D systems have been actively studied in the past,^{3–12,15–21} the role of strong disorder in 3D superconductors is just beginning to be addressed with a modern viewpoint,^{22,23} which naturally calls for explorations of suitable materials for such a study.

In this paper, we report that AgSnSe_2 , which is a low- T_c conventional superconductor having a cubic structure, offers an ideal playground for studying the effects of strong disorder in 3D superconductors. We show that one can synthesize high-quality samples of AgSnSe_2 presenting a very sharp superconducting transition, which indicates that morphologically the system is homogeneous; nonetheless, strong electron scatterings that are intrinsic to this system lead to an extremely type II superconductivity with the Ginzburg-Landau parameter κ_{GL} of as large as 55. This causes the emergence of a broad range of magnetic fields where the resistivity remains finite but is much smaller than the normal-state value as $T \rightarrow 0$, which is very much reminiscent of the behavior observed in disordered

2D superconductors^{11,12} or in quasi-2D systems like high- T_c cuprates.^{24,25} Furthermore, such an anomalous metallic state is found in the magnetic field range *above* the upper critical field determined thermodynamically from the specific heat. Since this anomalous state can be easily reached with the magnetic field of 3 T and the microscopic mechanism of superconductivity is well understood in conventional superconductors, future studies of AgSnSe_2 would help elucidate the roles of quantum phase fluctuations, which remain controversial to date.^{11–23}

II. AgSnSe_2 SUPERCONDUCTOR

The superconductivity in AgSnSe_2 was discovered by Johnston and Adrian²⁶ in 1977 as a possible valence-skipping superconductor. In valence-skipping compounds, the nominal valence state of a constituent element happens to be the skipped valence for that element. This characteristic has been of particular interest for superconductivity, since it may provide a means to realize the so-called negative- U mechanism to enhance the superconducting transition temperature T_c .²⁷ Well-known examples of such valence-skipping superconductors are $\text{BaBi}_{1-x}\text{Pb}_x\text{O}_3$,²⁸ $\text{Ba}_{1-x}\text{K}_x\text{BiO}_3$,²⁹ and $\text{Pb}_{1-x}\text{Ti}_x\text{Te}$.³⁰ In all these compounds, T_c is relatively high for their low carrier density. At the same time, valence fluctuations lead to significant electron scattering, making those superconductors highly disordered even though the matrix is homogeneous.

AgSnSe_2 adopts the face-centered cubic structure, in which the cation sites are randomly occupied by equal amount of Ag and Sn atoms. Since the nominal valence of Sn is $3+$, which coincides with its skipped valence state, the Sn ions should be separated into 1:1 mixture of Sn^{2+} and Sn^{4+} , and the chemical formula of this material can be more appropriately expressed as $(\text{Ag}^{1+})(\text{Sn}^{2+})_{0.5}(\text{Sn}^{4+})_{0.5}(\text{Se}^{2-})_2$, as evidenced by the measurements of the magnetic susceptibility²⁶ and the ^{119}Sn Mössbauer spectra.³¹ Despite the valence skipping nature and the carrier density of the order of 10^{22} cm^{-3} , its T_c of 4.7 K is not particularly high, which suggests that the negative- U mechanism is not at work here. Therefore, in this compound one can explore manifestations of strong disorder associated with valence fluctuations in the context

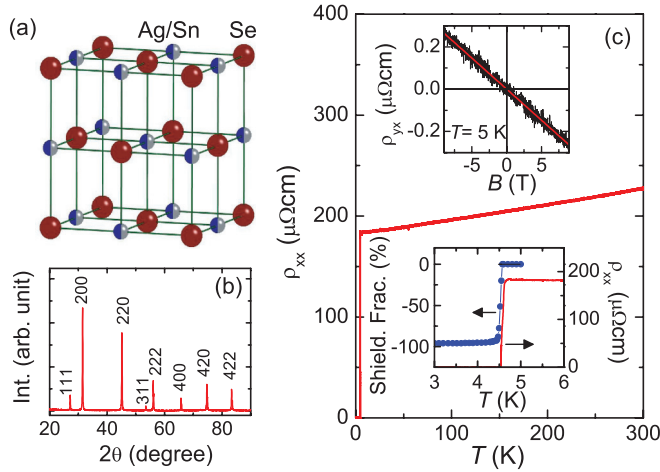


FIG. 1. (Color online) (a) Face-centered cubic structure of AgSnSe_2 . Note that Ag and Sn atoms are randomly distributed in the cation sites. (b) XRD pattern of the AgSnSe_2 sample. All the diffraction peaks can be well indexed using a cubic cell with the $Fm\bar{3}m$ space group. (c) Temperature dependence of ρ_{xx} of the AgSnSe_2 sample. Lower inset shows an enlarged view of the data near the superconducting transition for ρ_{xx} (right axis) and for the dc magnetic susceptibility measured upon zero-field-cooling (left axis, shown in terms of the shielding fraction). Upper inset shows the magnetic-field dependence of ρ_{yx} at 5 K; its slope gives $n_e = 2.0 \times 10^{22} \text{ cm}^{-3}$.

of conventional superconductivity without being bothered by strong electron interactions.

III. EXPERIMENTAL

We synthesized high-quality ingots of polycrystalline AgSnSe_2 by using a two-step method as described in Ref. 26. First, high-purity shots of Ag (99.999%), Sn (99.99%), and Se (99.999%) with the stoichiometric ratio of 1:1:2 were melted in sealed evacuated quartz tube at 800 °C for 48 h with intermittent shaking to ensure homogeneity, followed by quenching to room temperature. The quartz tube containing the melt-quenched ingot was subsequently annealed at 450 °C for 2 wk and then quenched into cold water. The structure of the resulting sample was characterized by powder x-ray diffraction (XRD). As can be seen in Fig. 1(b), the XRD pattern shows sharp diffraction peaks consistent with the face-centered cubic structure, giving the lattice parameter a of 5.675(1) Å, which agrees with the literature.²⁶

The ingot was cut into bar-shaped samples, and the temperature-dependent magnetization M under various magnetic fields was measured with a vibrating sample magnetometer (VSM), while the magnetization curves at fixed temperatures were measured with a commercial SQUID magnetometer (Quantum Design MPMS-1). The demagnetization effect was corrected for by considering the slab geometry.³² The resistivity ρ_{xx} and the Hall resistivity ρ_{yx} were measured by using a standard six-probe method where the contacts were made by spot-welding gold wires. The specific heat c_p was measured with a relaxation-time method using Quantum Design PPMS-9. For consistency reasons, all the data presented here were measured on exactly the same sample.

IV. BASIC CHARACTERIZATIONS

A. Transport properties and superconducting transition

Figure 1(c) shows the temperature dependence of ρ_{xx} , which exhibits only a weak metallic temperature dependence. This is qualitatively similar to that reported²⁶ for $\text{Ag}_{0.76}\text{Sn}_{1.24}\text{Se}_2$ and signifies the presence of intrinsically strong disorder that does not change much with the Ag/Sn ratio. As shown in the upper inset of Fig. 1(c), ρ_{yx} is linear in B and its slope at 5 K corresponds to an electron density n_e of $2.0 \times 10^{22} \text{ cm}^{-3}$. The superconducting transition in ρ_{xx} occurs sharply between 4.5 and 4.6 K, and the magnetic susceptibility shows the onset T_c of 4.55 K, which corresponds to the midpoint of the resistive transition. The superconducting shielding fraction achieves nearly 100% after the demagnetization correction. There is no resistivity upturn at low temperatures, giving no clear sign of Anderson localization.

B. Specific heat

Figure 2(a) shows the temperature dependencies of c_p/T measured under 0 and 9 T. Application of a 9 T field completely suppresses the superconductivity, enabling us to determine the phononic contribution and the normal-state parameters such as the electronic specific-heat coefficient γ_n and the effective mass m^* .³³ Figure 2(b) shows the temperature dependence of the electronic specific heat c_{el}/T in 0 T obtained by subtracting the phononic contribution determined from the 9 T data. One can see that c_{el}/T quickly approaches zero at low T , indicating a fully gapped nature. As for the precise temperature dependence, although the simple weak-coupling BCS model (dash-dotted line) fails to describe the c_{el}/T data, a modified BCS model³⁴ that allows the coupling constant $\alpha \equiv \Delta(0)/k_B T_c$ to vary [$\Delta(0)$ is the gap at 0 K] can fit our data well with $\alpha = 1.925$ (solid line), which is only slightly larger than the weak-coupling BCS value of 1.764.

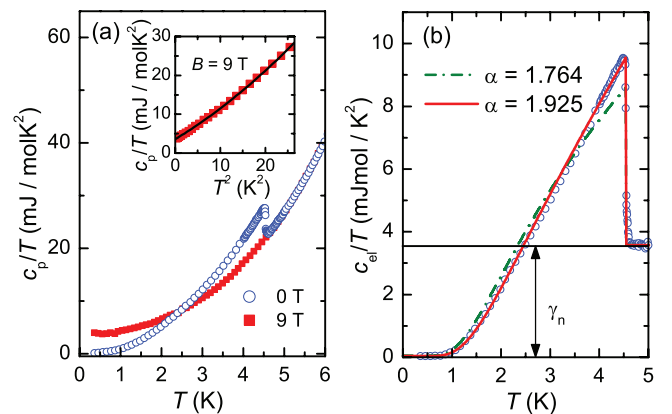


FIG. 2. (Color online) (a) Temperature dependencies of c_p/T measured in 0 and 9 T. Inset shows c_p/T plotted as a function of T^2 for the 9-T data, where the superconductivity is completely suppressed; the solid line presents the best fit to the data using the Debye model (see Ref. 33). (b) Temperature dependence of c_{el}/T in 0 T. The dash-dotted line is the calculated c_{el}/T curve given by the weak-coupling BCS theory; the solid line is the best fit using a modified BCS theory with $\alpha = 1.925$. The horizontal solid line denotes γ_n .

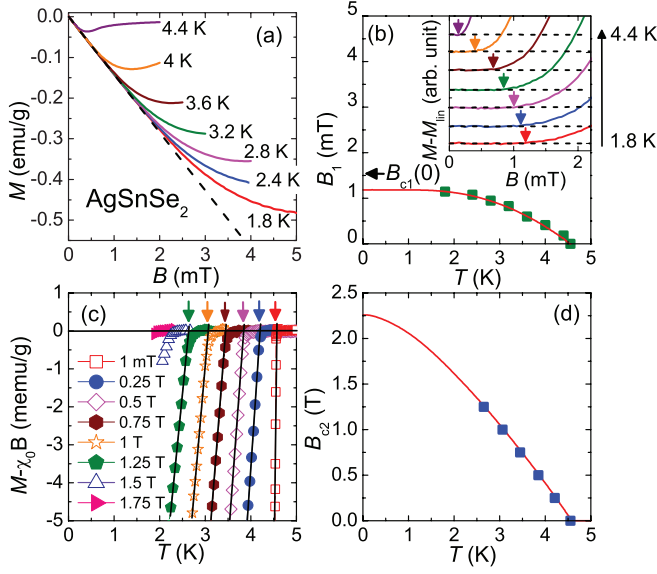


FIG. 3. (Color online) (a) $M(B)$ curves measured after zero-field cooling to various temperatures. The dashed line marks the initial linear behavior. (b) Plot of B_1 vs T ; the solid line is a fit to the data using the local dirty limit formula. The $B_{c1}(0)$ obtained after the demagnetization correction is marked by an arrow. Inset shows the B dependences of $\Delta M \equiv M - M_{\text{lin}}$, where M_{lin} denotes the initial Meissner contribution; the data are shifted vertically for clarity. The determined B_1 value for each temperature is shown by arrows. (c) Temperature dependencies of $M_{\text{sc}} \equiv M - \chi_0 B$ under various magnetic fields. The $T_c^{\text{Mag}}(B)$ values are indicated by arrows. (d) B_{c2}^{Mag} vs T phase diagram; the solid line is a WHH fit to the data.

Using m^* and α obtained from $c_p(T)$,³³ the Pippard coherence length ξ_0 can be estimated as $\xi_0 = \hbar^2(3\pi^2 n_e)^{1/3}/(\pi \alpha k_B T_c m^*) = 181$ nm. This is to be contrasted with the mean-free path $\ell = \hbar(3\pi^2)^{1/3}/(\rho_0 n_e^{2/3} e^2) = 0.9$ nm, where ρ_0 is the residual resistivity. This ℓ is less than $2a$ and is very short, pointing to the existence of strong scattering, which is consistent with the valence fluctuations of Sn. The ratio $\ell/\xi_0 = 0.005$ means that AgSnSe₂ is in the very dirty limit. Yet, $k_F \ell$ is estimated to be ~ 8 , and hence the system is still a good metal. Note that the estimations of m^* , k_F , ξ_0 , and ℓ in this paper are based on the free electron theory; once the band structure of AgSnSe₂ is known, those estimations can be made more accurate.

C. Critical fields

Figure 3 summarizes the results of the magnetization measurements to extract the values of the upper and lower critical fields. Figure 3(a) shows $M(B)$ curves measured after zero-field cooling to various temperatures. We define B_1 at each temperature as the value at which the $M(B)$ data deviates from its initial linear behavior, as can be more clearly seen in the inset of Fig. 3(b). Extrapolation³⁵ of the resulting $B_1(T)$ data to $T = 0$ K yields $B_1(0) = 1.18$ mT, which, after correcting for the demagnetization effect,³² gives the lower critical field at $T = 0$ K, $B_{c1}(0)$, of 1.58 mT.

Figure 3(c) shows the temperature dependencies of the magnetization near the superconducting transition under various magnetic fields. A paramagnetic background

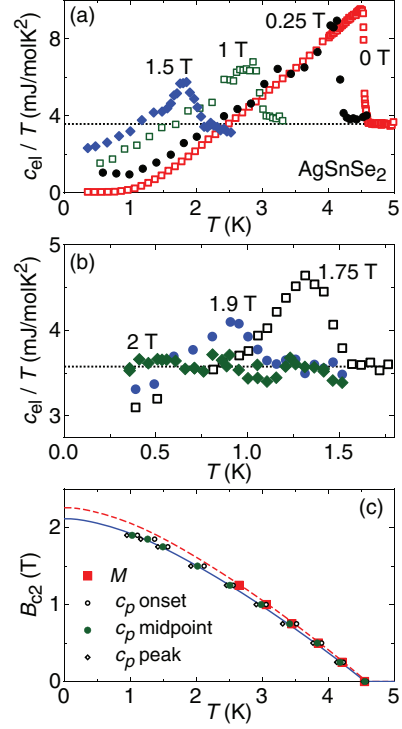


FIG. 4. (Color online) (a) and (b) Superconducting transition measured in the temperature dependence of the specific heat under various magnetic fields. (c) B_{c2}^{Cp} vs T phase diagram; the solid line is a WHH fit to the data. For comparison, $B_{c2}^{\text{Mag}}(T)$ and its WHH fitting are shown with filled squares and a dashed line, respectively.

with a temperature-independent susceptibility $\chi_0 = 4.2 \times 10^{-8}$ emu/g has been subtracted from the data,³⁶ and what is plotted is $M_{\text{sc}} \equiv M - \chi_0 B$. A gradual suppression of superconductivity with increasing magnetic field is evident. For each magnetic field, we determined the onset temperature of the transition, $T_c^{\text{Mag}}(B)$, from the intersection of the linear extrapolation of the $M_{\text{sc}}(T)$ data to the $M_{\text{sc}} = 0$ line, as indicated by the arrows in Fig. 3(c). The obtained $T_c^{\text{Mag}}(B)$ data shown in Fig. 3(d) give the temperature dependence of the magnetically determined upper critical field, $B_{c2}^{\text{Mag}}(T)$, which is extrapolated to $T = 0$ K using the Werthamer-Helfand-Hohenberg (WHH) theory³⁷ to yield $B_{c2}^{\text{Mag}}(0) = 2.26$ T.

To evaluate the upper critical field at low temperatures in a more direct way, we measured the superconducting transition in specific heat under various magnetic fields. Figure 4(a) shows representative data of c_{el}/T vs T measured in 0, 0.25, 1.0, and 1.5 T, where the superconducting transition is well resolved. In higher magnetic fields, the specific-heat anomaly becomes weaker, as shown in Fig. 4(b) for 1.75, 1.9, and 2.0 T; here the transition can still be seen in 1.9 T, but no clear anomaly is discernible at 2.0 T. These data demonstrate that the upper critical field is thermodynamically well defined in AgSnSe₂ at low temperature and that it lies around 2 T near $T = 0$ K.

To quantitatively analyze the superconducting transition in the specific-heat data, for each magnetic field we determined three characteristic temperatures: onset of the transition (below

which the specific heat grows), midpoint of the transition, and the peak in $c_p(T)$. It is useful to note that the transition width ΔT_c^{Cp} , which we define by the difference between the onset and peak temperatures, remains reasonably narrow with $\Delta T_c^{Cp} \lesssim 0.3$ K at all fields. We choose to use the midpoint of the specific-heat transition for defining the transition temperature $T_c^{Cp}(B)$ for each magnetic field, which in turn gives the temperature dependence of the upper critical field $B_{c2}^{Cp}(T)$.

The solid line in Fig. 4(c) is the fitting of the WHH theory to the $B_{c2}^{Cp}(T)$ data, which gives the $T = 0$ K value $B_{c2}^{Cp}(0)$ of 2.11 T. For comparison, we reproduced in Fig. 4(c) the $B_{c2}^{\text{Mag}}(T)$ data obtained from the magnetization measurements. The difference in the WHH fittings for the specific-heat and magnetization data is only 7%, which indicates that the two thermodynamical measurements are essentially consistent. In the following discussions, we take B_{c2}^{Cp} as the thermodynamically determined B_{c2} .

D. Superconducting parameters

Now we estimate various superconducting parameters of AgSnSe₂ by using $B_{c2}^{Cp}(0)$ as the zero-temperature upper critical field $B_{c2}(0)$. Note that since AgSnSe₂ has cubic symmetry, no anisotropy is expected. The Ginzburg-Landau (GL) coherence length $\xi_{\text{GL}}(0)$ is estimated as $\xi_{\text{GL}}(0) = \sqrt{\Phi_0/2\pi B_{c2}(0)} = 12.5$ nm, where $\Phi_0 = 2.07 \times 10^{-15}$ Wb is the flux quantum. Alternatively, one may also estimate ξ_{GL} from $\xi_{\text{GL}}(0) \simeq \sqrt{\xi_0 \ell}$ for dirty superconductors, which yields $\xi_{\text{GL}} \simeq 12.7$ nm. The consistency is gratifying. The equation³⁸ $B_{c1}(0)/B_{c2}(0) = (\ln \kappa_{\text{GL}} + 0.5)/(2\kappa_{\text{GL}}^2)$ gives the GL parameter $\kappa_{\text{GL}} = 55$, which in turn allows us to calculate the effective penetration depth $\lambda_{\text{eff}} = 685$ nm through $B_{c1}(0) = (\Phi_0/4\pi\lambda_{\text{eff}}^2)(\ln \kappa_{\text{GL}} + 0.5)$. This gives the London penetration depth $\lambda_L \simeq \lambda_{\text{eff}}\sqrt{\ell/\xi_0} = 48.3$ nm.

Since AgSnSe₂ is a very dirty superconductor, the superfluid density n_s is expected to be reduced by a factor of $\sim \ell/\xi_0$.³⁹ Indeed, the calculation of n_s based on $n_s = m^*/(\mu_0 e^2 \lambda_{\text{eff}}^2)$ yields $n_s \approx 9 \times 10^{19}$ cm⁻³, which is close to the estimation of $n_s \approx n_e(\ell/\xi_0) = 1 \times 10^{20}$ cm⁻³, reconfirming the applicability of the BCS theory to AgSnSe₂ and the soundness of our B_{c1} measurements, which can be adversely affected by flux pinning.

V. ANOMALOUS METALLIC STATE

A. Resistive transition in magnetic fields

Despite the conventional nature of the superconductivity in AgSnSe₂, nontrivial physics becomes evident when one looks at the magnetic-field-induced resistive transition at fixed temperatures (Fig. 5). One can easily see that the resistive transition is very sharp at temperatures close to T_c , but it becomes increasingly broader at lower temperatures. We determined the values of the magnetic field at which ρ_{xx} recovers a certain percentage of the normal-state resistivity ρ_N for each temperature, and denote them $B_{10\%}(T)$, $B_{50\%}(T)$, etc. We also determined the irreversibility field $B_{\text{irr}}(T)$ to mark the onset of a finite resistivity within our sensitivity limit, which corresponds to 0.15% of ρ_N . The results are shown in Fig. 6,

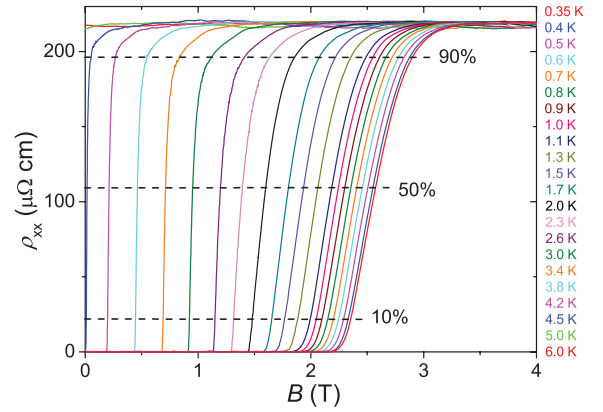


FIG. 5. (Color online) Magnetic-field-induced resistive transition measured at various temperatures. The level of ρ_{xx} that is used for determining $B_{10\%}$, $B_{50\%}$, and $B_{90\%}$ are indicated by dashed lines.

where we also plotted the thermodynamically-determined $B_{c2}(T)$ with a solid line.

Usually either $B_{50\%}(T)$ or $B_{90\%}(T)$ are considered to give a measure of the upper critical field.^{40,41} In the present case, for temperatures down to $T/T_c \sim 1/2$, $B_{50\%}(T)$ agrees reasonably well with the thermodynamically determined B_{c2} , but at lower temperatures the resistive transition occurs largely above B_{c2} . This means that at low temperature, there is a wide range of magnetic field above B_{c2} where the resistivity is finite but is noticeably smaller than ρ_N . The existence of such an anomalous metallic state above B_{c2} has never been documented for a conventional 3D superconductor, and this is the main finding of the present work. Note that the Pauli paramagnetic limit is estimated to be 8.4 T, which is well above the anomalous metallic regime observed here.

Similar broadening of the magnetic-field-induced resistive transition at low temperatures has been observed in high-temperature superconductors such as Bi₂Sr₂CuO_y,²⁴ Tl₂Ba₂CuO_y,²⁵ MgB₂,⁴² and Ba_{1-x}K_xBiO₃.⁴³ This phenomenon is generally believed to be caused by enhanced vortex fluctuations and the resulting vortex liquid phase due to a short coherence length that is inherent to high-temperature superconductors. In light of this common belief, the present observation in AgSnSe₂ is striking. Here the coherence length

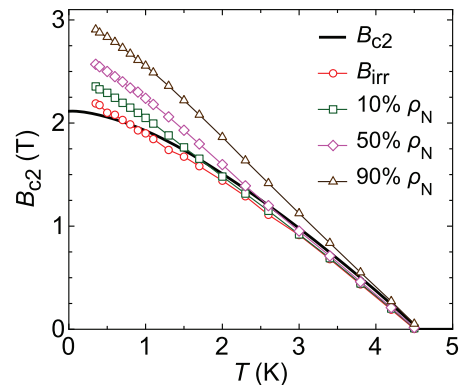


FIG. 6. (Color online) Plots of B_{irr} , $B_{10\%}$, $B_{50\%}$, and $B_{90\%}$ obtained from the resistive transition data, together with B_{c2} determined thermodynamically from specific-heat measurements (solid line).

is not so short, 12.1 nm, and the system is 3D, both of which work against strong vortex fluctuations. Therefore, our result calls for a reinterpretation of the low-temperature broadening of the magnetic-field-induced resistive transition.

B. Quantum phase fluctuations

To understand the above results, an interesting possibility is the scenario proposed by Spivak, Oreto, and Kivelson¹³ that the strong disorder leads to formations of superconducting “puddles” that are Josephson coupled to each other, and quantum fluctuations of the relative phase between those puddles give rise to a broad range of magnetic fields where the resistivity remains finite and smaller than ρ_N as $T \rightarrow 0$. If this is indeed the case, our data give evidence for the important role of quantum phase fluctuations in disordered 3D conventional superconductors. Since the superconductivity mechanism is well understood here (as opposed to the case of high-temperature superconductors) and the required magnetic field to access the quantum fluctuation regime is low (only ~ 3 T), AgSnSe₂ provides a convenient platform for studying the role of quantum fluctuations in the magnetic-field-induced superconductor-to-metal transition.

Another anomalous behavior observed here is that at low temperatures, not only $B_{90\%}$ but also B_{irr} shows little tendency toward saturation. A similar behavior was previously observed in strongly disordered amorphous superconductors⁴¹ and was discussed to be due to the weak-localization effect.⁴⁴ However,

the discrepancy between the resistive transition and the thermodynamically determined B_{c2} makes the conclusion of those old studies^{41,44} questionable. Hence, the physical meaning of the resistive transition in disordered superconductors had better be reconsidered by taking into account the important role of quantum phase fluctuations.

VI. SUMMARY

We have fully characterized the AgSnSe₂ superconductor where its valence-skipping nature leads to intrinsically strong electron scattering without any obvious enhancement of T_c . At low temperature, we observed an anomalous broadening of the magnetic-field-induced resistive transition, which occurs largely above the thermodynamically-determined B_{c2} . This means the existence of an anomalous metallic state above B_{c2} where quantum phase fluctuations associated with a magnetic-field-induced superconductor-to-metal transition are likely to be playing an important role. This makes AgSnSe₂ a useful platform for studying the role of quantum fluctuations in 3D disordered superconductors.

ACKNOWLEDGMENTS

We thank S. A. Kivelson for illuminating discussions. This work was supported by JSPS (NEXT Program and KAKENHI 24740237), MEXT (Innovative Area “Topological Quantum Phenomena” KAKENHI 22103004), and AFOSR (AOARD 124038).

*y_ando@sanken.osaka-u.ac.jp

¹P. W. Anderson, *J. Phys. Chem. Solids* **11**, 26 (1959).

²R. Balian and N. R. Werthamer, *Phys. Rev.* **131**, 1553 (1963).

³M. P. A. Fisher, *Phys. Rev. Lett.* **65**, 923 (1990).

⁴D. B. Haviland, Y. Liu, and A. M. Goldman, *Phys. Rev. Lett.* **62**, 2180 (1989).

⁵A. F. Hebard and M. A. Paalanen, *Phys. Rev. Lett.* **65**, 927 (1990).

⁶M. A. Paalanen, A. F. Hebard, and R. R. Ruel, *Phys. Rev. Lett.* **69**, 1604 (1992).

⁷S. Tanda, S. Ohzeki, and T. Nakayama, *Phys. Rev. Lett.* **69**, 530 (1992).

⁸M. P. A. Fisher and D. H. Lee, *Phys. Rev. B* **39**, 2756 (1989).

⁹T. Pang, *Phys. Rev. Lett.* **62**, 2176 (1989).

¹⁰M. P. A. Fisher, G. Grinstein, and S. M. Girvin, *Phys. Rev. Lett.* **64**, 587 (1990).

¹¹N. Mason and A. Kapitulnik, *Phys. Rev. Lett.* **82**, 5341 (1999).

¹²M. A. Steiner, G. Boebinger, and A. Kapitulnik, *Phys. Rev. Lett.* **94**, 107008 (2005).

¹³B. Spivak, P. Oreto, and S. A. Kivelson, *Phys. Rev. B* **77**, 214523 (2008).

¹⁴M. V. Feigel'man, L. B. Ioffe, V. E. Kravtsov, and E. Cuevas, *Ann. Phys. (NY)* **325**, 1390 (2010).

¹⁵J. M. Valles, Jr., R. C. Dynes, and J. P. Garno, *Phys. Rev. Lett.* **69**, 3567 (1992).

¹⁶Y. Liu, D. B. Haviland, B. Nease, and A. M. Goldman, *Phys. Rev. B* **47**, 5931 (1993).

¹⁷S. Doniach, *J. Phys. Chem. Solids* **56**, 1601 (1995).

¹⁸G. Sambandamurthy, L. W. Engel, A. Johansson, and D. Shahar, *Phys. Rev. Lett.* **92**, 107005 (2004).

¹⁹Y. Dubi, Y. Meir, and Y. Avishai, *Nature (London)* **449**, 876 (2007).

²⁰M. D. Stewart, Jr., A. J. Yin, J. M. Xu, and J. M. Valles, Jr., *Science* **318**, 1273 (2007).

²¹B. Sacépé, T. Dubouchet, C. Chapelier, M. Sanquer, M. Ovadia, D. Shahar, M. Feigel'man, and L. Ioffe, *Nat. Phys.* **7**, 239 (2011).

²²M. Mondal, S. Kumar, M. Chand, A. Kamlapure, G. Saraswat, G. Seibold, L. Benfatto, and P. Raychaudhuri, *Phys. Rev. Lett.* **107**, 217003 (2011).

²³M. Chand, G. Saraswat, A. Kamlapure, M. Mondal, S. Kumar, J. Jesudasan, V. Bagwe, L. Benfatto, V. Tripathi, and P. Raychaudhuri, *Phys. Rev. B* **85**, 014508 (2012).

²⁴M. S. Osofsky, R. J. Soulen, Jr., S. A. Wolf, J. M. Broto, H. Rakoto, J. C. Ousset, G. Coffe, S. Askenazy, P. Pari, I. Bozovic, J. N. Eckstein, and G. F. Virshup, *Phys. Rev. Lett.* **71**, 2315 (1993).

²⁵A. P. Mackenzie, S. R. Julian, G. G. Lonzarich, A. Carrington, S. D. Hughes, R. S. Liu, and D. C. Sinclair, *Phys. Rev. Lett.* **71**, 1238 (1993).

²⁶D. C. Johnston and H. Adrian, *J. Phys. Chem. Solids* **38**, 355 (1977).

²⁷C. M. Varma, *Phys. Rev. Lett.* **61**, 2713 (1988).

²⁸A. W. Sleight, J. L. Gillson, and P. E. Bierstedt, *Solid State Commun.* **17**, 27 (1975).

²⁹R. J. Cava, B. Batlogg, J. J. Krajewski, R. Farrow, L. W. Rupp, Jr., A. E. White, K. Short, W. F. Peck, and T. Kometani, *Nature (London)* **332**, 814 (1988).

³⁰S. A. Nemov and Y. I. Ravich, *Phys. Usp.* **41**, 735 (1998).

³¹F. S. Nasredinov, S. A. Nemov, V. F. Masterov, and P. P. Seregin, *Phys. Solid State* **41**, 1741 (1999).

³²E. H. Brandt, *Phys. Rev. B* **60**, 11939 (1999).

³³As can be seen in the inset of Fig. 2(a), the 9 T data below 5 K can be well described by the Debye model $c_p/T = \gamma_n + A_3T^2 + A_5T^4$, where γ_n is the normal-state electronic specific-heat coefficient and A_i ($i = 3, 5$) denote the coefficients of the phononic contribution. The obtained parameters are $\gamma_n = 3.5$ mJ/molK², $A_3 = 0.7$ mJ/molK⁴, and $A_5 = 0.009$ mJ/molK⁶. The A_3 value gives the Debye temperature $\Theta_D = 220$ K via $\Theta_D = (12\pi^4 n R / 5 A_3)^{1/3}$ with $n = 4$ and $R = 8.314$ J/molK. In addition, if one assumes a single spherical Fermi surface, the effective mass m^* can be estimated as $m^* = 3\hbar^2\gamma_n / (V_{\text{mol}}k_B^2(3\pi^2n_e)^{1/3}) \simeq 1.5m_e$, where $V_{\text{mol}} = 55$ cm³/mol and m_e is the free electron mass.

³⁴H. Padamsee, J. E. Neighbor, and C. A. Shiffman, *J. Low Temp. Phys.* **12**, 387 (1973).

³⁵We fit the $B_1(T)$ curve with $B_1 \propto 1/\lambda_{\text{eff}}^2 \propto [\Delta(T)/\Delta(0)] \tanh(\Delta(T)/2k_B T)$ for the local dirty limit,³⁹ where λ_{eff} is the effective penetration depth.

³⁶The positive χ_0 is probably due to the presence of a very small amount of paramagnetic impurities.

³⁷N. R. Werthamer, E. Helfand, and P. C. Hohenberg, *Phys. Rev. B* **147**, 295 (1966).

³⁸C.-R. Hu, *Phys. Rev. B* **6**, 1756 (1972).

³⁹M. Tinkham, *Introduction to Superconductivity* (McGraw-Hill, New York, 1975).

⁴⁰Y. Ando, G. S. Boebinger, A. Passner, L. F. Schneemeyer, T. Kimura, M. Okuya, S. Watauchi, J. Shimoyama, K. Kishio, K. Tamasaku, N. Ichikawa, and S. Uchida, *Phys. Rev. B* **60**, 12475 (1999).

⁴¹M. Tenhover, W. L. Johnson, and C. C. Tsuei, *Solid State Commun.* **38**, 53 (1981).

⁴²P. Szabo, P. Samuely, A. G. M. Jansen, T. Klein, J. Marcus, D. Fruchart, and S. Miraglia, *Physics C* **369**, 250 (2002).

⁴³P. Samuely, P. Szabo, T. Klein, A. G. M. Jansen, J. Marcus, C. Escribe-Filippini, and P. Wyder, *Europhys. Lett.* **41**, 207 (1998).

⁴⁴L. Coffey, K. Levin, and K. A. Muttalib, *Phys. Rev. B* **32**, 4382 (1985).